Colletofragarone A2 and Colletoins A–C from a Fungus *Colletotrichum* sp. Decrease Mutant p53 Levels in Cells

Yusaku Sadahiro,[†] Yuki Hitora,[†] and Sachiko Tsukamoto[†,*]

[†] Graduate School of Pharmaceutical Sciences, Kumamoto University, Kumamoto 862-0973, Japan

p53 is frequently mutated in tumor cells, and mutant p53 (mut p53) accumulates in cells to promote cancer progression, invasion, and metastasis and it is attracting attention as a target for cancer therapies. In this study, we used immunofluorescence staining of Saos-2 cells harboring doxycycline-inducible $p53^{R175H}$ [Saos-2 ($p53^{R175H}$) cells] to search for compounds from natural sources that can target mut p53 and found an extract of *Colletotrichum* sp. (13S020). Bioassay-guided fractionation of the extract afforded a known polyketide, colletofragarone A2 (**1**), and three new analogues, colletoins A–C (**2**–**4**). The relative and absolute configurations of **1** were determined by the spectroscopic method and DFT calculation. Compounds **1** and **2** inhibited the growth of Saos-2 ($p53^{R175H}$) cells and decreased mut p53 in the cells.

The tumor suppressor p53 is a transcription factor activated by DNA damage and cellular stress, which regulates the transcription of genes for apoptosis, cell cycle arrest, metabolism, and senescence.[1,2] Mutations of p53 are found in more than 50% of tumors, resulting in the loss of its tumor suppressor function.[3,4] Furthermore, it has been reported that missense mutations of p53 not only cause it to lose its tumor suppressor function but also result in the gain of new oncogenic functions (gain-of-function).[5] The types of p53 mutations can be mainly categorized as either DNA contact or structural mutants.[3,6] DNA contact mutants such as R248W and R273H maintain the same conformation as wild-type p53 (wt p53), but their DNA binding affinity is weakened. Structural mutations such as R175H, R245S, and R282W cause local or global structural disruption, resulting in the loss of the original function of the tumor suppressor.

In tumor cells, mutant p53 (mut p53) levels are higher than that of wt p53, and the half-life of mut p53 is more than 24 h compared with less than 30 min for wt p53.[7] Mut p53 is stabilized by HSP90 and HDAC6,[8,9] causing it to accumulate in tumors, progressing tumorigenesis.[10] Recently, cancer therapeutics targeting mut p53 have attracted much attention, and compounds that convert the structure of mut p53 to a wt-like conformation or induce its degradation have been developed.[11,12] PRIMA-1,[13] MIRA-1,[14] arsenic trioxide,[15] and phenethyl isothiocyanate (PEITC)[16] have been reported to change the conformation of mut p53, restoring its tumor suppressor function. A phase III clinical trial of APR-246,[17] a methylated derivative of PRIMA-1, in combination with azacitidine is ongoing for *TP53*-mutated myelodysplastic syndromes.[18] HSP90 inhibitors, geldanamycin[19] and gambogic acid,[20] and an HDAC

inhibitor, suberoylanilide hydroxamic acid (SAHA),[9] have been reported to destabilize mut p53 and inhibit tumor growth. Therefore, agents targeting mut p53 show promise as therapeutics for tumor regression.

To discover new natural products that can target mut p53, we first tested the effects of fungal extracts against Saos-2 cells harboring doxycycline-inducible $p53^{R175H}$, Saos-2 ($p53^{R175H}$) cells,[21] because compounds that decrease mut p53 are expected to reduce tumor growth.[22] Next, hits were screened by immunofluorescent staining to determine their effects on mut p53 levels in the cells. Using this two-stage screening system, we evaluated 2,311 fungal samples and found that the extract of *Colletotrichum* sp. (13S020) decreased cellular mut p53. Bioassay-guided fractionation of the extract afforded colletofragarone A2[23] (**1**) and three new analogues, colletoins A–C (**2**–**4**). Here, we describe the isolation, structure elucidation, and biological activities of **1**–**4**.

RESULTS AND DISCUSSION

First, 2,311 fungal extracts were evaluated for their growth inhibitory activity on Saos-2 ($p53^{R175H}$) cells (Figure 1A). Hits (166 extracts) were subjected to immunofluorescence assay for mut p53. Briefly, Saos-2 ($p53^{R175H}$) cells were treated with extracts and incubated for 6 h. After fixation, cells were incubated with an anti-mut p53 antibody (PAb240), and the amount of mut p53 protein in the cells was evaluated by immunofluorescence staining. The ratio of fluorescence intensities was represented by an F_T (fluorescence of test samples)/F_C (fluorescence of control) score. PEITC, which is reported to induce

conformational changes in $p53^{R175H}$,[16] has an F_T/F_C score of 0.43 at 5 μM and was used as a positive control (Figure 1B). Among the 166 samples, seven extracts with F_T/F_C scores smaller than 0.5 were selected as hits (Figure 1A). Among these, the extract of *Colletotrichum* sp. showed an F_T/F_C score of 0.42 (Figure 1B), and the compounds within this extract that decreased $p53^{R175H}$ were purified.

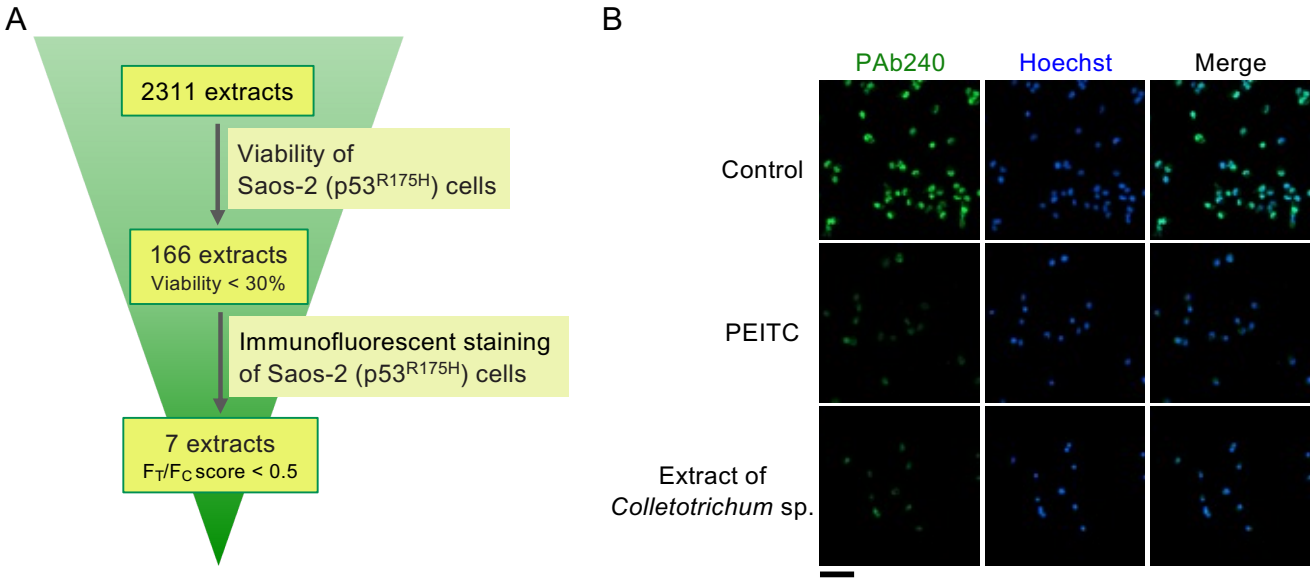

Figure 1. (A) Screening of fungal extracts that reduce $p53^{R175H}$ in Saos-2 ($p53^{R175H}$) cells. (B) Immunofluorescence staining of Saos-2 ($p53^{R175H}$) cells. Cells were treated with 5 μM PEITC as a positive control or the extract of *Colletotrichum* sp. and stained by immunofluorescence using an anti-mut p53 antibody (PAb240) or Hoechst 33342. The scale bar represents 100 μm.

The fungus *Colletotrichum* sp. was grown on rice medium, and its *n*-BuOH extract was partitioned between *n*-BuOH and H_2O. The organic layer was concentrated and partitioned between *n*-hexane and 90% MeOH−H_2O. Bioassay-guided purification of the *n*-hexane and 90% MeOH–H_2O fractions by MPLC and HPLC afforded a known polyketide, colletofragarone A2[23] (**1**), and three new analogues, colletoins A–C (**2**–**4**).

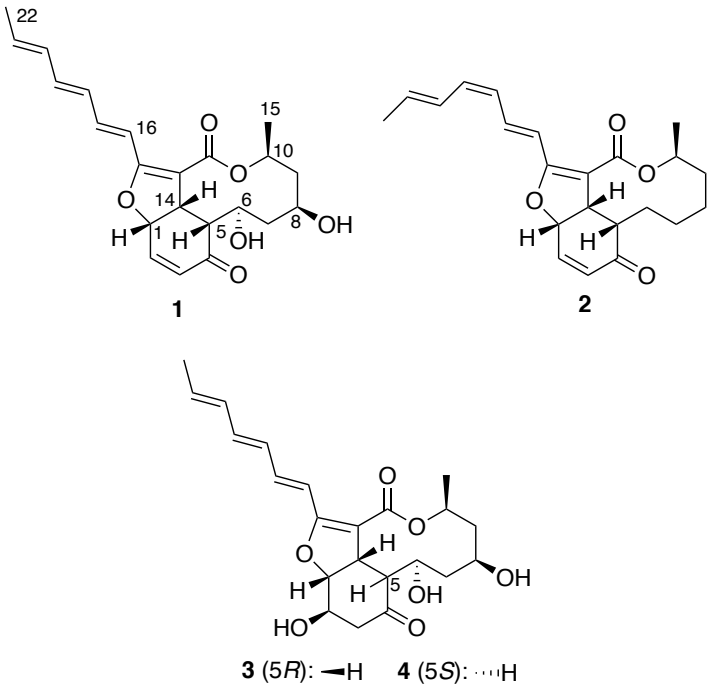

Compound **1** was identified as colletofragarone A2 by comparing the spectroscopic data (Table 1) with those in the literature.[23] Although NOE correlations among H-1, H-5, and H-14 suggested that these protons were located on the same face, the relative configurations of C-6, C-8, and C-10 in the 10-membered lactone and the absolute configuration of **1** had not been determined.[23] From the spectroscopic data, the large coupling constants of H-5/H-6 (J = 9.9 Hz) indicated the anti-relationships of these vicinal protons. NOE correlations of H-7β/H-9β, H-7β/H-14, and H-9β/H-15 indicated β-orientations of these protons, and in turn, those of H-6/H-10 and H-8/H-10 indicated that they were on the α-face (Figure 2A). Thus, the relative configuration of **1** was assigned to be 1*S**,5*R**,6*R**,8*S**,10*S**,14*S**. The absolute configuration of **1** was then determined from the calculated ECD spectrum. Indications of a positive Cotton effect in the calculated spectrum of 1*S*,5*R*,6*R*,8*S*,10*S*,14*S*-**1** showed the absolute configuration of

1 (Figure 2B).

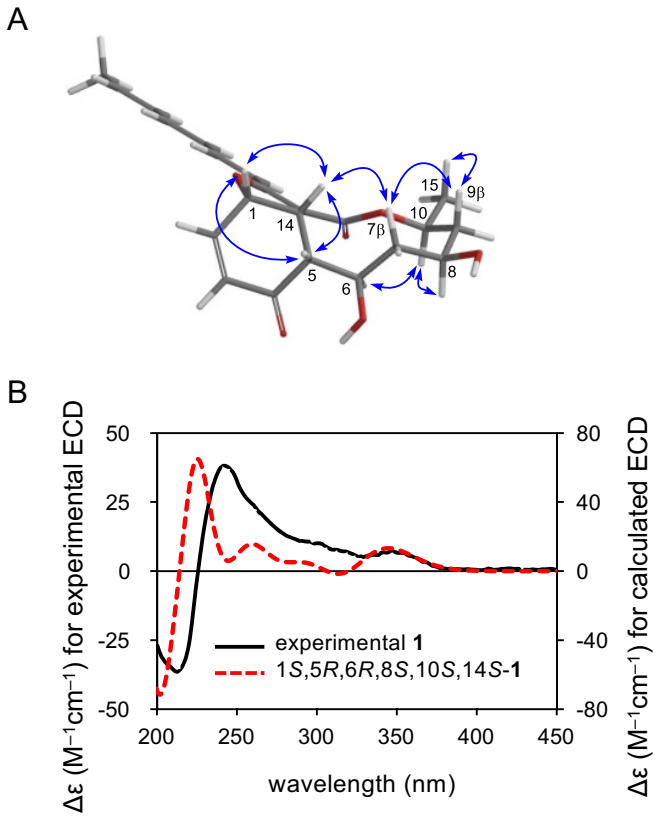

Figure 2. (A) Stable conformation of **1** and key NOEs. (B) Experimental ECD spectrum (MeOH) of **1** and calculated ECD spectrum of 1*S*,5*R*,6*R*,8*S*,10*S*,14*S*-**1** with BHandHLYP/TZVP.

Table 1. ^{13}C and ^{1}H NMR data for **1** and **2** in $CDCl_3/CD_3OD$ (9:1).

1			**2**		
no.	δ_C, type	δ_H (*J* in Hz)	no.	δ_C, type	δ_H (*J* in Hz)
1	76.7, CH	5.39, dd (9.2, 3.5)	1	75.9, CH	5.31, br d (9.4)
2	140.3, CH	6.45, dd (10.1, 3.4)	2	139.9, CH	6.54, br d (9.3)
3	131.5, CH	6.04, d (10.1)	3	130.8, CH	6.04, m
4	202.7, C		4	200.0, C	
5	52.1, C	2.64, dd (9.9, 5.4)	5	45.8, C	2.58, br s
6	69.8, CH_2	3.59, br t (9.9, 9.0)	6a	25.4, CH_2	1.93, br s
			6b		0.99, br s
7α	42.6, CH_2	1.31, dd (14.0, 9.5)	7a	23.7, CH_2	1.57, br s
7β		2.26, dd (14.0, 9.0)	7b		1.31, br s
8	69.3, CH_2	3.79 [a]	8a	23.1, CH_2	1.71 [a]
			8b		1.25, br s
9α	44.5, CH_2	1.89, br d (14.2)	9a	32.7, CH_2	1.67 [a]
9β		1.67 [a]	9b		1.41, br s
10	71.0, CH	4.56, m	10	72.7, CH	4.84, br s
11	165.2, C		11	165.8, C	
12	104.8, C		12	106.1, C	
13	161.1, C		13	161.1, C	
14	44.3, CH	4.18, dd (9.2, 5.4)	14	43.1, CH	4.23, br s
15	21.5, CH_3	1.27, d (6.0)	15	19.5, CH_3	1.16, d (5.8)
16	116.0, CH	6.30, d (15.5)	16	117.3, CH	6.49, d (15.3)
17	137.7, CH	6.66, dd (15.5, 11.0)	17	131.7, CH	7.11, dd (11.3, 15.3)
18	128.9, CH	6.04, m	18	125.6, CH	5.83, dd (11.3, 11.5)
19	139.0, CH	6.27, dd (14.9, 11.0)	19	134.8, CH	6.03, m
20	131.5, CH	6.00, dd (15.1, 11.0)	20	126.8, CH	6.45, m
21	133.8, CH	5.74, dq (15.1, 6.7)	21	133.6, CH	5.73, m
22	18.3, CH_3	1.67, d (6.7)	22	18.2, CH_3	1.67, d (6.0)

[a] Coupling patterns of the designated signals were not clear as they overlapped other signals in the columns.

The molecular formula of **2** was determined to be $C_{22}H_{26}O_4$ by HRESIMS, which indicated the lack of two oxygen atoms with respect to **1**. The ^{1}H and ^{13}C NMR data of **2** were similar to those of **1** (Table 1), except for the absence of two oxygen-bearing methine signals. Detailed analysis of 2D NMR data indicated that **2** has the same carbon framework as **1** and the methines at C-6 and C-8 are replaced with methylenes in **2** (Figure 3A). NOE correlations H-16/H-18, H-17/H-20, H-19/H-21, and H-20/H_3-22 showed a *trans*-*cis*-*trans*-conjugated triene system (Figure 3B). The relative configuration of the

cyclohexenone unit was the same as that of **1**, as shown by NOE correlations among H-1, H-5, and H-14 (Figure 3B). Spectroscopic analysis of the relative configuration of C-10 was unsuccessful because of the broad ^{1}H NMR spectrum of **2**. NMR measurement at a higher temperature in DMSO-d_6 also failed because of the decomposition of the sample. From the biosynthetic perspective, **1** and **2** were presumed to possess the same stereochemistry at C-10. The absolute configuration of **2** was indicated to be 1*S*,5*S*,10*S*,14*S* by comparing the experimental and calculated ECD spectra (Figure 3C).

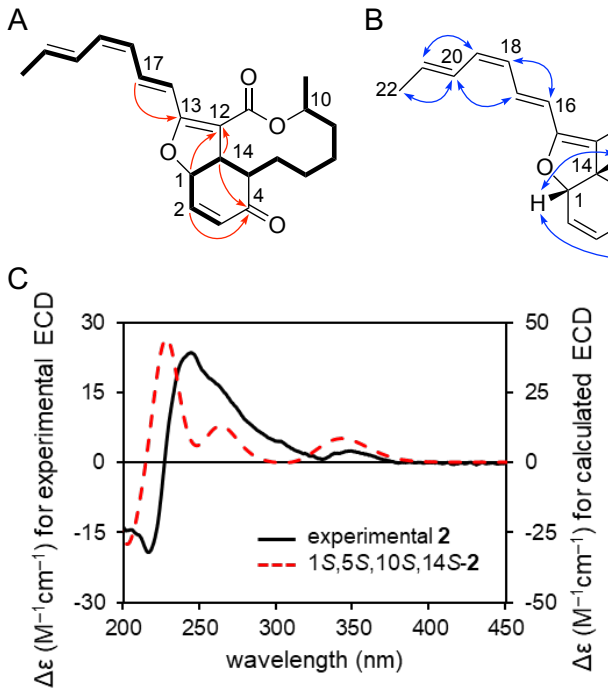

Figure 3. (A) COSY (bold lines) and key HMBC (arrows) correlations of **2**. (B) Key NOE (arrows) correlations of **2**. (C) Experimental ECD spectrum (MeOH) of **2** and calculated ECD spectrum of 1*S*,5*S*,10*S*,14*S*-**2** with BHandHLYP/TZVP.

Compounds **3** and **4** have identical molecular formulas of $C_{22}H_{28}O_7$, which is an H_2O unit more than that of **1**. Their ^{1}H and ^{13}C NMR spectra were almost superimposable. The HSQC spectrum indicated

that **3** has an oxymethine at δ_H 4.35/δ_C 66.6 and a methylene at δ_H 2.47 and 2.37/δ_C 43.3 instead of the 1,2-disubstituted olefin in **1** (Table 2). Interpretation of COSY and HMBCs from H-3β to C-4, from H-5 to C-3 and C-4, and from H-14 to C-4 indicated the presence of a cyclohexanone moiety in **3** (Figure 4A), which clearly showed the positions of the oxymethine and methylene at C-2 and C-3, respectively. NOE correlations of H-16/H-18, H-17/H-19, H-18/H-20, H-19/H-21, and H-20/H_3-22 showed a *trans*-*trans*-*trans*-conjugated triene system (Figure 4A), and NOEs on the cyclohexanone showed that H-1, H-5, and H-14 are on the same face (Figure 4B). The large coupling constant of H-5/H-6 (J = 9.5 Hz) indicated their anti-relationship. Moreover, NOE correlations of H-6/H-10 and H-8/H-10 showed that H-6, H-8, and H-10 are on the α-face (Figure 4B). The relative configuration of C-2 was examined on the stable conformers obtained by computational calculation. The observed coupling constants were 4.4 ($J_{H\text{-}2,H\text{-}3\alpha}$) and 0 ($J_{H\text{-}2,H\text{-}3\beta}$) Hz (Table 2), and the calculated data were 5.0 ($J_{H\text{-}2,H\text{-}3\alpha}$) and 1.3 ($J_{H\text{-}2,H\text{-}3\beta}$) Hz for 2*R**-**3** and 10.5 ($J_{H\text{-}2,H\text{-}3\alpha}$) and 5.7 ($J_{H\text{-}2,H\text{-}3\beta}$) Hz for 2*S**-**3**, respectively (Figure 5), suggesting that **3** adopts the 2*R** configuration. DP4 scores[24] of the ^{13}C NMR chemical shifts were 82.7 and 17.3% for 2*R**- and 2*S**-**3**, respectively, which support the 2*R**-configuration. As with **1** and **2**, signs of the Cotton effect calculated for 1*R*,2*R*,5*R*,6*R*,8*S*,10*S*,14*S*-**3** indicated the absolute configuration of **3** (Figure S25).

Analysis of 2D NMR data indicated that **4** has the same planer structure as **3**. Although H-5 showed NOEs with H-14 in **3**, H-5 of **4** revealed a NOE correlation with H-8 but not with H-14, indicating that **4** is the 5-epimer of **3** (Figure 4B). To determine the relative configuration of C-2, the calculated ^{13}C NMR chemical shifts of 2*R**- and 2*S**-**4** were analyzed. The DP4 score of 2*R**-**4** was 100%, whereas

the score of 2*S**-**4** was 0%. Furthermore, the root mean square of the deviation (RMSD) value[25] of 2*R**-**4** (1.6 ppm) was smaller than that of 2*S**-**4** (2.7 ppm), indicating the 2*R**-configuration (Table S2). The absolute configuration of **4** was shown to be 1*R*,2*R*,5*S*,6*R*,8S,10*S*,14*S* by comparing the experimental and calculated ECD spectra (Figure S26).

Table 2. ^{13}C and ^{1}H NMR data for **3** and **4** in $CDCl_3/CD_3OD$ (9:1).

	3		**4**	
no.	δ_C, type	δ_H (*J* in Hz)	δ_C, type	δ_H (*J* in Hz)
1	81.6, CH	4.86, dd (9.8, 3.4)	80.2, CH	4.80, dd (10.1, 3.0)
2	66.6, CH	4.35, m	66.5, CH	4.30, br d (3.0)
3α	43.3, CH_2	2.47, dd (19.1, 4.4)	42.5, CH_2	2.55, br dd (17.7, 3.0)
3β		2.37, br d (19.1)		2.50, dd (17.7, 3.0)
4	214.7, C		212.9, C	
5	53.8, CH	3.27, dd (9.5, 6.5)	54.7, CH	2.02, br s
6	68.9, CH	3.43, dd (8.8, 9.5)	71.8, CH	4.24, dd (12.6, 3.9)
7α	43.9, CH_2	1.32, dd (14.0, 8.8)	44.5, CH_2	1.54, m
7β		2.20, dd (14.0, 9.1)		2.23, br t (13.7)
8	69.7, CH	3.70, br d (9.1)	66.9, CH	3.29, dd (9.8, 5.8)
9α	44.2, CH_2	1.86, br d (14.3)	44.9, CH_2	1.71, br d (4.4)
9β		1.69 [a]		1.78, m
10	70.5, CH	4.63, m	71.5, CH	4.57, m
11	164.9, C		164.2, C	
12	104.2, C		109.0, C	
13	164.9, C		163.1, C	
14	43.3, CH	3.96, dd (9.8, 6.5)	36.3, CH	3.70, d (10.1)
15	21.3, CH_3	1.24, d (6.0)	21.0, CH	1.24, d (5.7)
16	116.7, CH	6.61, d (15.5)	116.6, CH	6.69, d (15.5)
17	138.7, CH	6.66, dd (15.5, 10.7)	138.5, CH	6.76, dd (15.5, 10.8)
18	129.1, CH	6.06, dd (14.8, 10.7)	128.9, CH	6.09, dd (14.9, 10.8)
19	139.3, CH	6.27, dd (14.8, 10.8)	139.2, CH	6.29, dd (14.9, 10.7)
20	131.6, CH	6.01, m	131.3, CH	6.01, dd (14.8, 10.7)
21	134.0, CH	5.74, m	133.8, CH	5.75, dq (14.8, 6.7)
22	18.3, CH_3	1.67, d (6.2)	18.1, CH_3	1.68, d (6.7)

[a] Coupling pattern of the designated signal was not clear because of overlap with H_3-22.

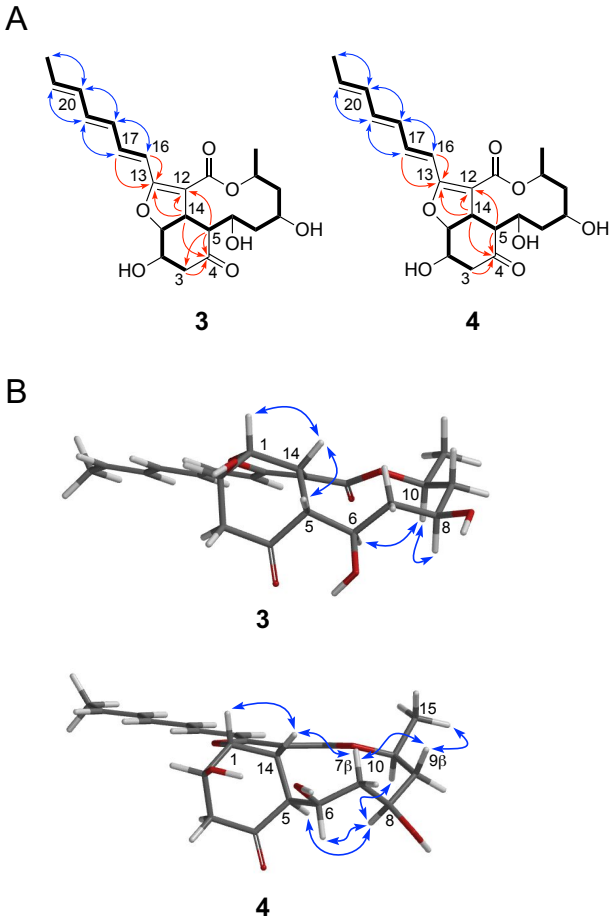

Figure 4. (A) COSY (bold lines), key HMBC (red arrows), and key NOE correlations (blue arrows) of **3** and **4**. (B) Key NOE (arrows) correlations of **3** and **4** in the stable conformations.

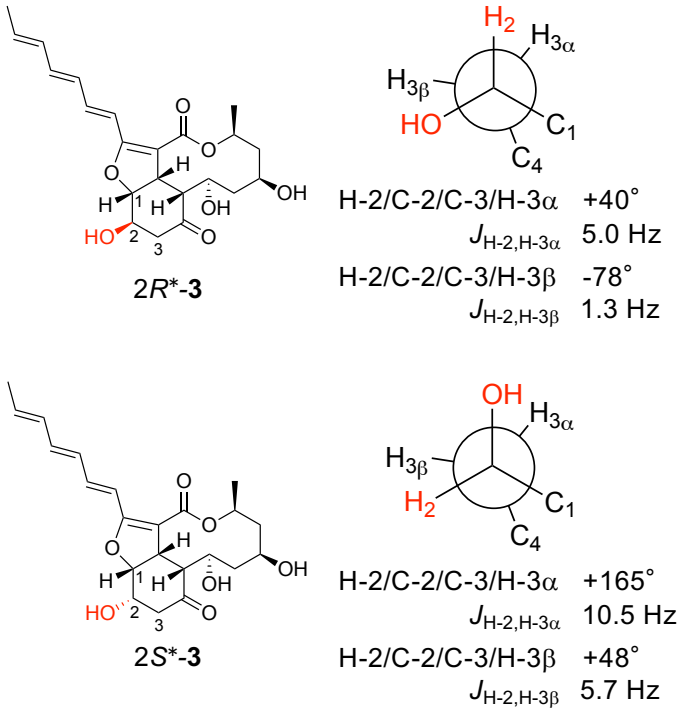

Figure 5. The dihedral angles of H-2/C-2/C-3/H-3α and H-2/C-2/C-3/H-3β and their coupling constants in 2*R**- and 2*S**-**3**.

Compounds **1** and **2** exhibited cytotoxic activity against Saos-2 ($p53^{R175H}$) cells, with IC_{50} values of 0.35 and 0.36 μM, respectively, whereas the activities of **3** and **4** were weak (IC_{50}, 21 and 12 μM, respectively). These data indicated that the α,β-unsaturated carbonyl group is involved in cytotoxicity. The effects of **1** and **2** on mut p53 were investigated by immunofluorescence staining with an anti-mut p53 antibody (PAb240). Fluorescence intensities of the cells treated with 2 μM **1** or **2** decreased, with F_T/F_C scores of 0.40 and 0.57, respectively (Figure 6), indicating that **1** and **2** reduced the level of mut p53 in the cells.

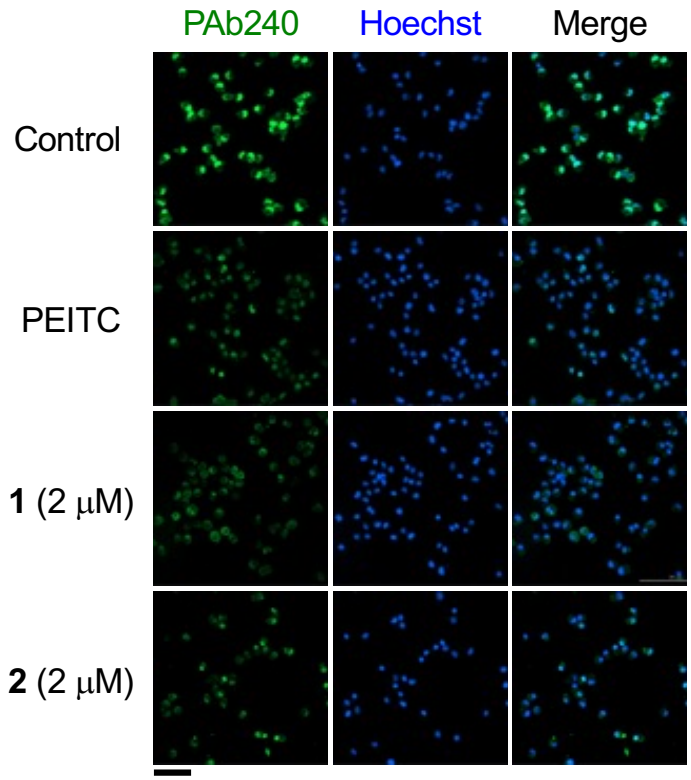

Figure 6. Immunofluorescence of Saos-2 ($p53^{R175H}$) cells. Cells were treated with 5 μM PEITC as a positive control, 2 μM **1**, or 2 μM **2** and stained by immunofluorescence using an anti-mut p53 antibody (PAb240) or Hoechst 33342. The scale bar represents 100 μm.

In this study, we used immunofluorescence staining of Saos-2 ($p53^{R175H}$) cells to search for natural products that can target mut p53. Bioassay-guided purification of the extract of *Colletotrichum* sp. afforded **1** and **2** as the active compounds, which exhibited potent cytotoxicity against Saos-2 ($p53^{R175H}$) cells and decreased the level of mut p53 in the cells. Originally, **1** was isolated as a germination self-inhibitor from *Colletotrichum fragariae* by Ueno and colleagues.[23] Subsequently, the group of Lindquist and Gunatilaka reported that **1** inhibited the proliferation of human glioma cell lines (LN428, LN827, and U87) and activated the heat shock factor.[26] The mechanism of suppression of mut p53 by **1** is now being investigated in our laboratory. Small molecules targeting mut p53 are expected to be emerging

anticancer agents, and the technique of immunofluorescence staining of mut p53, which we used in this study, may facilitate the discovery of new anticancer drugs.

EXPERIMENTAL SECTION

General Experimental Procedures. Optical rotations were measured on a JASCO DIP-1000 polarimeter in $CHCl_3$/MeOH (9:1) or MeOH, UV spectra on a JASCO V-550 spectrophotometer in MeOH, ECD spectra on a JASCO J-820 spectropolarimeter in MeOH, IR spectra on a Perkin Elmer Frontier FT-IR spectrophotometer, and ^{1}H and ^{13}C NMR spectra on a Bruker Avance I 600 NMR spectrometer in $CDCl_3/CD_3OD$ (9:1). Chemical shifts were referenced to the residual solvent peaks (δ_H 7.24 and δ_C 77.0 for $CDCl_3$). ESI-HRMS data were recorded on a Waters Xevo G2-XS QTof mass spectrometer. Preparative MPLC was performed on a Biotage Iolera I, and LC-MS was performed on a Shimadzu LC-20AD solvent delivery system and interfaced to a Bruker amaZon speed mass spectrometer. The preparative HPLC system comprised a Waters 515 HPLC pump and Waters 2489 UV/visible detector. Fluorescent microscopic images were obtained using a BioTek Cytation 1 cell imaging multi-mode reader and a Leica DMi8 microscope. Saos-2 ($p53^{R175H}$) cells were kindly provided by Professor Peter Kaiser of the University of California, Irvine.[21]

Fungal Strain Identification. The fungal strain 13S020 was isolated from a leaf of an unidentified plant at Aso, Kumamoto Prefecture, Japan, in 2013. The strain was identified from ITS sequence; a 566

base pair ITS sequence had 100% sequence identity to that of *Colletotrichum* sp. (GenBank accession No. MZ930390).

Cultivation of the Fungus Screened. Fungus screened were cultivated on malt extract agar or rice medium. Malt extract agar composed of 2.0% malt extract, 0.5% peptone, 0.5% peptone and 1.5% agar was used for seed medium. Fungi, cultivated on the seed medium (20 mL) in petri dishes (ϕ90 × 15 mm) at 25 °C for 7 d, were cultured on production medium with the same composition at 25 °C for 14 d. The fungal cultures were extracted with 8 mL of EtOH, and the portions (3 mL) were evaporated. The dried extracts were dissolved in 70 μL of DMSO and filtrated through a 0.45 μm filter. Rice medium composed of 2.0% glucose, 0.2% yeast extract, 0.5% peptone, 0.2% KH_2PO_4, 0.05% $MgSO_4·7H_2O$, and 1.5% agar was used for seed medium. Fungi were cultivated on the seed medium (20 mL) in petri dishes (ϕ90 × 15 mm) at 25 °C for 7 d. Solid rice was used as the production medium. Rice (5 g) in a 50 mL Falcon tube with 5 mL H_2O containing 0.25% KH_2PO_4, 0.75% K_2HPO_4, 0.03% CH_3COONH_4, 0.02% $(NH_4)_2SO_4$, 0.005% $NaNO_3$, 0.05% $MgSO_4·7H_2O$, 0.001% $FeSO_4·7H_2O$, 0.001% $ZnSO_4·7H_2O$, 0.005% $CuSO_4·5H_2O$, and 0.005% $MnSO_4·H_2O$ was autoclaved at 121 °C for 30 min. Fungi grown on the seed medium were cultured on the rice at 25 °C for 20 d. The fungal cultures were extracted with 10 mL of *n*-BuOH, and the extracts were partitioned between *n*-BuOH and H_2O. The *n*-BuOH soluble fractions were partitioned between *n*-hexane and 90% MeOH−H_2O, and the 90% MeOH−H_2O fractions was evaporated and dissolved in DMSO (10 mg/mL).

Cultivation of the Fungus *Colletotrichum* sp. (13S020). The production medium was prepared with

rice (100 g) in a plastic container (W17 × D22 cm × H9 cm) with 100 mL water containing the ingredients described above and autoclaved at 121 °C for 30 min. The fungus grown on the seed medium was cultured on the rice (10 containers) at 25 °C for 20 d.

Extraction and Isolation. The fungal culture was extracted with *n*-BuOH, and the extract was partitioned between *n*-BuOH and H_2O. The *n*-BuOH soluble fraction was partitioned between *n*-hexane and 90% MeOH–H_2O, and the 90% MeOH–H_2O fraction was evaporated to yield 18 g of extract. A portion (3 g) of the extract was subjected to normal-phase MPLC (Purif-Pack®-EX SI-50 um, size: 60; SHOKO SCIENCE Co., Ltd.) with a linear gradient system using 0–30% *n*-hexane–EtOAc and a stepwise gradient system using CH_2Cl_2, CH_2Cl_2–MeOH (49:1, 19:1, 9:1, 7:3, and 1:1), and MeOH to yield 18 fractions (Frs. A1–A18). Fraction A8 (368 mg), eluted by CH_2Cl_2/MeOH (9:1), was fractionated by normal-phase MPLC (Purif-Pack®-EX ODS-50 um, size: 60) with a stepwise gradient system using *n*-hexane–EtOAc (9:1), *n*-hexane–EtOAc (3:1, 1:1, 1:3, and 1:9), EtOAc, CH_2Cl_2–MeOH (19:1, 9:1, and 4:1), and MeOH. The EtOAc eluate (110.2 mg) was further separated by reverse-phase MPLC (Purif-Pack®-EX ODS-50 um, size: 20) with a linear gradient system (10–100% MeOH–H_2O for 15 min and MeOH for 8.5 min). A portion (20 mg) of the fraction eluted at 11–12 min (48.3 mg) was purified by HPLC (Luna 5u phenyl-hexyl, 21.2 × 250 mm; Phenomex Inc.) with 75% MeOH–H_2O to yield **1** (9.3 mg). Fractions A10 and A11, eluted with CH_2Cl_2–MeOH (9:1), were combined (94.4 mg) and subjected to reversed-phase MPLC (Purif-Pack®-EX ODS-50 um, size: 20) with a stepwise gradient system using 40, 60, 80, and 90% MeOH–H_2O. The 80% MeOH–H_2O eluate was purified by HPLC (Luna 5u phenyl-

hexyl, 21.2 × 250 mm) with 70% MeOH–H_2O to yield **3** (4.28 mg) and **4** (1.84 mg). The *n*-hexane fraction (20 g) was subjected to normal-phase MPLC (Purif-Pack®-EX SI-50 um, size: 60) with a stepwise gradient system using *n*-hexane–CH_2Cl_2 (7:3, 1:1, 3:7, and 1:9), CH_2Cl_2, CH_2Cl_2–MeOH (19:1 and 9:1), and MeOH. A portion of the fraction eluted with *n*-hexane–CH_2Cl_2 (3:7, 540 mg) was subjected to normal-phase HPLC (YMC-pack R&D D-SIL-5, 20 × 250 mm; YMC Co., Ltd.) with *n*-hexane–CH_2Cl_2 (1:9) and purified by size exclusion HPLC (Asahipak GS-310P column, 21.5 × 500 mm; Asahi Chemical Industry Co., Ltd.) with CH_2Cl_2 to afford **2** (23.9 mg).

*Colletofragarone A2 (**1**):* White powder; $[\alpha]^{28.5}_D$ +417.5 (*c* 1.32, $CHCl_3$/MeOH (9:1)); UV (MeOH) λ_{max} (log ε) 340 (4.33) and 250 (3.64); ECD (MeOH) λ_{max} (Δε) 346 (+7.5), 329 (+5.1), 242 (+38.4), and 212 (–36.5) nm; ^{1}H and ^{13}C NMR data, Table 1; HRESIMS *m/z* 387.1789 $[M + H]^+$ (calcd for $C_{22}H_{27}O_6$, 387.1803).

*Colletoin A (**2**):* White solid; $[\alpha]^{26.9}_D$ +269.6 (*c* 1.32, $CHCl_3$/MeOH (9:1)); UV (MeOH) λ_{max} (log ε) 336 (4.38) and 264 (3.68); ECD (MeOH) λ_{max} (Δε) 347 (+2.5), 330 (+0.6), 244 (+23.6), and 216 (–19.3) nm; IR (film) ν_{max}, 2930, 2856, 1688, 1618, 1357, 1312, 1249, 1112, 1069, and 967 cm^{-1}; ^{1}H and ^{13}C NMR data, Table 1; HRESIMS *m/z* 355.1903 $[M + H]^+$ (calcd for $C_{22}H_{27}O_4$, 355.1904).

*Colletoin B (**3**):* White solid; $[\alpha]^{26.9}_D$ +83.9 (*c* 0.67, MeOH); UV (MeOH) λ_{max} (log ε) 344 (4.34) and 248 (3.73); ECD (MeOH) λ_{max} (Δε) 329 (+1.3), 264 (–0.5), and 242 (+1.7) nm; IR (film) ν_{max} 3383, 2926, 1697, 1616, 1371, 1311, 1248, 1101, 1049, and 1001 cm^{-1}; ^{1}H and ^{13}C NMR data, Table 2; HRESIMS *m/z* 405.1901 $[M + H]^+$ (calcd for $C_{22}H_{29}O_7$, 405.1908).

Colletoin C (4): White solid; $[\alpha]^{28.5}_{D}$ +84.3 (*c* 0.67, MeOH); UV (MeOH) λ_{max} (log ε) 344 (4.24) and 250 (3.90); ECD (MeOH) λ_{max} (Δε) 325 (+0.6), 282 (–1.0), and 246 (+3.7) nm; IR (film) ν_{max} 3341, 2928, 1695, 1607, 1370, 1310, 1250, 1211, 1100, 1049, and 1002 cm^{-1}; ^{1}H and ^{13}C NMR data, Table 2; HRESIMS *m/z* 405.1913 $[M + H]^+$ (calcd for $C_{22}H_{29}O_7$, 405.1908).

Conformational Analysis and Chemical Shift Calculations for Models 2*R- and 2*S**-3 and 2*R**- and 2*S**-4.** Conformational analyses and chemical shift calculations were carried out for models 2*R**- and 2*S**-**3** and 2*R**- and 2*S**-**4** as previously described using Spartan'18 software (Wave function Inc.) on a commercially available PC (operating system, Windows 10 Education; CPU, Intel® Core™ i7-8700K 3.70 GHz; RAM, 64 GB).[27] The obtained chemical shifts were corrected using the Boltzmann distribution to give calculated ^{13}C NMR chemical shifts. The obtained ^{13}C NMR chemical shifts were evaluated by RMSD against the experimental data of **3** or **4** (Table 2). In the DP4 analysis, the parameters shown in Goodman's procedure (^{13}C: σ = 2.306 ppm and ν = 11.38) were used.[24]

ECD Calculations of 1–4. Conformational analyses were carried out as previously described using Spartan'18 software with slight modification. Briefly, conformational searches were conducted using MMFF as the force field, and the obtained stable conformers were optimized by the Hartree-Fock with 3-21G and further optimized by the density functional theory method with B3LYP/6-31G*. ECD calculations were conducted with Gaussian16 (Revision C.01 by Gaussian) on a PC (operating system, CentOS Linux 7; CPU, Intel® Core™ i9-9900 3.10 GHz; RAM, 64 GB). ECD calculations were

performed at the BHandHLYP/TZVP level, and the calculated ECD spectra were obtained after wavelength correction with the experimental UV absorption peak at 340 nm.

Cell Culture. Saos-2 ($p53^{R175H}$) cells were cultured in DMEM (high glucose, 044-29765; Fujifilm Wako Pure Chemical Corp.) containing 10% fetal bovine serum (FBS-12A; Capricorn Scientific), 100 U/mL penicillin, 10 μg/mL streptomycin, and 250 μg/mL hygromycin B at 37 °C in an atmosphere of 5% CO_2.

3-(4,5-Dimethylthiazol-2-yl)-2,5-diphenyltetrazolium Bromide (MTT) Viability Test of Fungal Extracts. The MTT assay was conducted as previously described with slight modifications.[28] Briefly, Saos-2 ($p53^{R175H}$) cells were suspended in DMEM (high glucose) supplemented with 1.0 μg/mL doxycycline. The cell suspension (0.2 mL, 10,000 cells/mL) was seeded into a 96-well plate in the presence of the extracts (1 μL) and incubated at 37 °C in an atmosphere of 5% CO_2 for 3 d. The medium was then replaced with 50 μL of MTT solution (500 μg/mL in medium), and the cells were incubated under the same conditions for 3 h. After addition of 150 μL of DMSO, the absorbance at 570 nm was measured.

MTT Viability Test for Isolated Compounds. Saos-2 ($p53^{R175H}$) cells treated with doxycyclin were seeded into a 96-well plate (0.2 mL, 10,000 cells/mL) and incubated overnight. Sample solution (1 μL) in DMSO was added to each well and cells were incubated for 3 d. The medium was then replaced with 50 μL of MTT solution (500 μg/mL in medium), and the cells were incubated under the same conditions

for 3 h. After addition of 150 μL of DMSO, the absorbance at 570 nm was measured.

Immunofluorescent Staining. Saos-2 ($p53^{R175H}$) cells were treated with doxycycline, seeded into a 96-well plate (0.2 mL, 25,000 cells/mL), and incubated overnight. Sample solution (1 μL) in DMSO was added to each well and incubated for 2 h for the isolated compounds or 6 h for the extracts. Cells were washed once with PBS and fixed with formaldehyde (4.0%) at room temperature for 15 min. Fixed cells were washed two times with PBS and treated with 0.5% Triton X-100 at room temperature for 5 min. Cells were washed two times with PBS containing 0.1% Tween-20 (PBST) and blocked with 10% goat serum at 4 °C overnight. Cells were washed two times with PBST and incubated with the primary antibody, anti-mut p53 (PAb240, 1:300; Santa Cruz Biotechnology, Inc.), at 4 °C overnight. After washing with PBST twice, the cells were incubated with the secondary antibody, Alexa Fluor 488-conjugated goat anti-mouse IgG (1:400; Thermo Fisher Scientific K.K.) or Hoechst 33342 (1:1,000; Dojindo Laboratories), at room temperature for 2 h. Cells were washed three times with PBST and replaced with 100 μL of PBS. Fluorescent microscopic images were acquired using a BioTek Cytation 1 cell imaging multi-mode reader and processed using Gen5 data analysis software (BioTek Instruments, Inc.).

ASSOCIATED CONTENT

Supporting Information

The Supporting Information is available free of charge at https://pubs.acs.org/doi/ 10.1021/acs.jnatprod.xxxxxxx.

NMR spectra of **1**–**4**; ECD spectra of **3** and **4**; Experimental ^{13}C NMR data of **3** and **4** (PDF).

AUTHOR INFORMATION

Corresponding Author

Sachiko Tsukamoto – *Department of Natural Medicines, Graduate School of Pharmaceutical Sciences, Kumamoto University, 5-1 Oe-honmachi, Kumamoto 862-0973, Japan;* http://orcid.org/0000-0002-7993-381X; E-mail: sachiko@kumamoto-u.ac.jp

Authors

Yusaku Sadahiro – *Department of Natural Medicines, Graduate School of Pharmaceutical Sciences, Kumamoto University, 5-1 Oe-honmachi, Kumamoto 862-0973, Japan.*

Yuki Hitora – *Department of Natural Medicines, Graduate School of Pharmaceutical Sciences, Kumamoto University, 5-1 Oe-honmachi, Kumamoto 862-0973, Japan.* http://orcid.org/0000-0003-4271-2543.

Notes

The authors declare no competing financial interest.

ACKNOWLEDGMENT

This work was supported by JSPS KAKENHI Grant Numbers JP20H03396 (S.T.) and JP20K16026 (Y.H.).

REFERENCES

(1) Levine, A. J.; Oren, M. *Nat. Rev. Cancer* **2009**, *9*, 749–758.

(2) Kastenhuber, E. R.; Lowe, S. W. *Cell* **2017**, *170*, 1062–1078.

(3) Bykov, V. J. N.; Eriksson, S. E.; Bianchi, J.; Wiman, K. G. *Nat. Rev. Cancer* **2018**, *18*, 89–102.

(4) Bouaoun, L.; Sonkin, D.; Ardin, M.; Hollstein, M.; Byrnes, G.; Zavadil, J.; Olivier, M. *Hum. Mutat*. **2016**, *37*, 865–876.

(5) Alvarado-Ortiz, E.; de la Cruz-López, K. G.; Becerril-Rico, J.; Sarabia-Sánchez, M. A.; Ortiz-Sánchez, E.; García-Carrancá, A. *Front. Cell Dev. Biol*. **2021**, *8*, 607670.

(6) Ang, H. C.; Joerger, A. C.; Mayer, S.; Fersht, A. R. *J. Biol. Chem*. **2006**, *281*, 21934–21941.

(7) Nagata, Y.; Anan, T.; Yoshida, T.; Mizukami, T.; Taya, Y.; Fujiwara, T.; Kato, H.; Saya, H.; Nakao, M. *Oncogene* **1999**, *18*, 6037–6049.

(8) Peng, Y.; Chen, L.; Li, C.; Lu, W.; Chen, J. *J. Biol. Chem*. **2001**, *276*, 40583–40590.

(9) Li, D.; Marchenko, N. D.; Moll, U. M. *Cell Death Differ*. **2011**, *18*, 1904–1913.

(10) Muller, P.; Hrstka, R.; Coomber, D.; Lane, D. P.; Vojtesek, B. *Oncogene* **2008**, *27*, 3371–3383.

(11) Zhu, G.; Pan, C.; Bei, J.-X.; Li, B.; Liang, C.; Xu, Y.; Fu, X. *Front. Oncol*. **2020**, *10*, 595187.

(12) Parrales, A.; Iwakuma, T. *Front. Oncol*. **2015**, *5*, 288.

(13) Bykov, V. J. N.; Issaeva, N.; Shilov, A.; Hultcrantz, M.; Pugacheva, E.; Chumakov, P.; Bergman, J.; Wiman, K. G.; Selivanova, G. *Nat. Med*. **2002**, *8*, 282–288.

(14) Bykov, V. J. N.; Issaeva, N.; Zache, N.; Shilov, A.; Hultcrantz, M.; Bergman, J.; Selivanova, G.; Wiman, K. G. *J. Biol. Chem*. **2005**, *280*, 30384–30391.

(15) Chen, S.; Wu, J.-L.; Liang, Y.; Tang, Y.-G.; Song, H.-X.; Wu, L.-L.; Xing, Y.-F.; Yan, N.; Li, Y.-T.; Wang, Z.-Y.; Xiao, S.-J.; Lu, X.; Chen, S.-J.; Lu, M. *Cancer Cell* **2021**, *39*, 225–239.e8.

(16) Aggarwal, M.; Saxena, R.; Sinclair, E.; Fu, Y.; Jacobs, A.; Dyba, M.; Wang, X.; Cruz, I.; Berry, D.; Kallakury, B.; Mueller, S. C.; Agostino, S. D.; Blandino, G.; Avantaggiati, M. L.; Chung, F.-L. *Cell Death Differ*. **2016**, *23*, 1615–1627.

(17) Bykov, V. J. N.; Zache, N.; Stridh, H.; Westman, J.; Bergman, J.; Selivanova, G.; Wiman, K. G. *Oncogene* **2005**, *24*, 3484–3491.

(18) Maslah, N.; Salomao, N.; Drevon, L.; Verger, E.; Partouche, N.; Ly, P.; Aubin, P.; Naoui, N.; Schlageter, M.-H.; Bally, C.; Miekoutima, E.; Rahmé, R.; Lehmann-Che, J.; Ades, L.; Fenaux, P.; Cassinat, B.; Giraudier, S. *Haematologica* **2020**, *105*, 1539–1551.

(19) Whitesell, L.; Sutphin, P.; An, W. G.; Schulte, T.; Blagosklonny, M. V.; Neckers, L. *Oncogene* **1997**, *14*, 2809–2816.

(20) Wang, J.; Zhao, Q.; Qi, Q.; Gu, H.-Y.; Rong, J.-J.; Mu, R.; Zou, M.-J.; Tao, L.; You, Q.-D.; Guo, Q.-L. *J. Cell Biochem*. **2011**, *112*, 509–519.

(21) Wassman, C. D.; Baronio, R.; Demir, Ö.; Wallentine, B. D.; Chen, C.-K.; Hall, L. V.; Salehi, F.; Lin, D.-W.; Chung, B. P.; Hatfield, G. W.; Chamberlin, A. R.; Luecke, H.; Lathrop, R. H.; Kaiser, P.; Amaro, R. E. *Nat. Commun*. **2013**, *4*, 1407.

(22) Ubby, I.; Krueger, C.; Rosato, R.; Qian, W.; Chang, J.; Sabapathy, K. *Oncogene* **2019**, *38*, 3415–3427.

(23) Inoue, M.; Takenaka, H.; Tsurushima, T.; Miyagawa, H.; Ueno, T. *Tetrahedron Lett*. **1996**, *37*, 5731–5734.

(24) Smith, S. G.; Goodman, J. M. *J. Am. Chem. Soc*. **2010**, *132*, 12946–12959.

(25) Inose, K.; Tanaka, S.; Tanaka, K.; Hashimoto, M. *J. Org. Chem.* **2021**, *86*, 1505–1515.

(26) Santagata, S.; Xu, Y. M.; Wijeratne, E. M. K.; Kontnik, R.; Rooney, C.; Perley, C. C.; Kwon, H.; Clardy, J.; Kesari, S.; Whitesell, L.; Lindquist, S.; Gunatilaka, A. A. L. *ACS Chem. Biol*. **2012**, *7*, 340–349.

(27) Torii, M.; Kato, H.; Hitora, Y.; Angkouw, E. D.; Mangindaan, R. E. P.; de Voogd, N. J.; Tsukamoto, S. *J. Nat. Prod*. **2017**, *80*, 2536–2541.

(28) Tsukamoto, S.; Yamanokuchi, R.; Yoshitomi, M.; Yoshitomi, M.; Sato, K.; Ikeda, T.; Rotinsulu, H.; Mangindaan, R. E. P.; de Voogd, N. J.; van Soest, R. W. M.; Yokosawa, H. *Bioorg. Med. Chem. Lett*. **2010**, *20*, 3341–3343.

Table of Contents